Evaluation of the Main MPPT Techniques for Photovoltaic Applications

Moacyr Aureliano Gomes de Brito, Luigi Galotto, Jr., Leonardo Poltronieri Sampaio, Guilherme de Azevedo e Melo, and Carlos Alberto Canesin, *Senior Member, IEEE*

***Abstract*—This paper presents evaluations among the most usual maximum power point tracking (MPPT) techniques, doing meaningful comparisons with respect to the amount of energy extracted from the photovoltaic (PV) panel [tracking factor (TF)] in relation to the available power, PV voltage ripple, dynamic response, and use of sensors. Using MatLab/Simulink and dSPACE platforms, a digitally controlled boost dc–dc converter was implemented and connected to an Agilent Solar Array E4350B simulator in order to verify the analytical procedures. The main experimental results are presented for conventional MPPT algorithms and improved MPPT algorithms named IC based on proportional–integral (PI) and perturb and observe based on PI. Moreover, the dynamic response and the TF are also evaluated using a user-friendly interface, which is capable of online program power profiles and computes the TF. Finally, a typical daily insulation is used in order to verify the experimental results for the main PV MPPT methods.**

***Index Terms*—Photovoltaic (PV) energy, PV maximum power point (MPP) tracker (MPPT) algorithms, PV power profile, PV tracking factor (TF).**

I. Introduction

THE growing energy demand coupled with the possibility of reduced supply of conventional fuels, evidenced by petroleum crisis, along with growing concerns about environmental conservation, has driven research and development of alternative energy sources that are cleaner, are renewable, and produce little environmental impact. Among the alternative sources, the electrical energy from photovoltaic (PV) cells is currently regarded as a natural energy source that is more useful, since it is free, abundant, clean, and distributed over the Earth and participates as a primary factor of all other processes of energy production on Earth. Moreover, in spite of the phenomena of reflection and absorption of sunlight by the atmosphere, it is estimated that solar energy incident on the Earth's surface is on the order of ten thousand times greater than the world energy consumption. A great advantage of PV cells is the reduction of carbon dioxide emissions. By the year 2030, the annual reduction rate of CO_2 due to the usage of PV cells may be around 1 Gton/year, which is equivalent to India's total emissions in 2004 or the emission of 300 coal plants [1]. According to experts, the energy obtained from PV cells will become the most important alternative renewable energy source until 2040 [2]. In this context, the concept of distributed energy generation became a real and present technical possibility, promoting various research works and standardizations in the world. Despite all the advantages presented by the generation of energy through PV cells, the efficiency of energy conversion is currently low, and the initial cost for its implementation is still considered high; thus, it becomes necessary to use techniques to extract the maximum power from these panels, in order to achieve maximum efficiency in operation. Under uniform solar irradiation conditions, PV panels exhibits a unique operating point where PV power is maximized. The PV power characteristic is nonlinear, as shown in Fig. 1—considering a single PV cell, which varies with the level of solar irradiation and temperature, which make the extraction of maximum power a complex task, considering load variations. Thus, in order to overcome this problem, several methods for extracting the maximum power have been proposed in the literature [3]–[21], and a careful comparison of these methods can result in important information for the design of these systems. Therefore, this paper aims to assess the main maximum power point (MPP) tracking (MPPT) techniques through models in MatLab/Simulink and experimental results, doing depth comparisons among them with regard to the voltage ripple, start-up of the method, tracking factor (TF), and usage of sensors. It should be informed

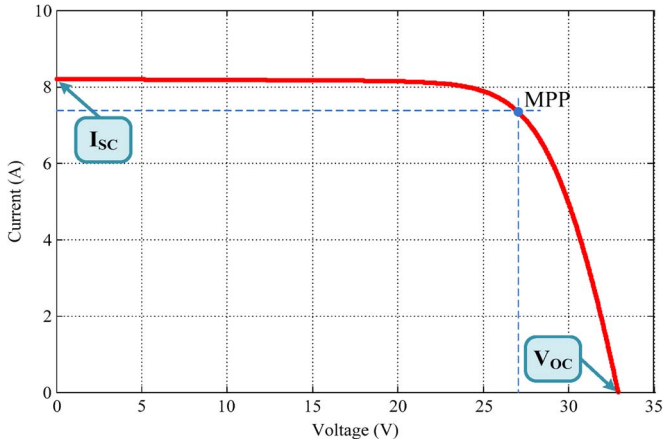

Fig. 1. PV current-versus-voltage characteristic.

Manuscript received August 24, 2011; revised December 19, 2011 and March 12, 2012; accepted April 18, 2012. Date of publication May 7, 2012; date of current version October 16, 2012.

M. A. G. de Brito, L. P. Sampaio, G. A. e Melo, and C. A. Canesin are with the Power Electronics Laboratory (LEP), São Paulo State University (UNESP), Ilha Solteira-SP 15385-000, Brazil (e-mail: moa.brito@gmail.com; leo_sjrp@yahoo.com; guiamelo@gmail.com; canesin@dee.feis.unesp.br).

L. Galotto, Jr., is with Federal University of Mato Grosso do Sul (UFMS), Cidade Universitária, Campo Grande 79004-970, Brazil (e-mail: lgalotto@gmail.com).

Color versions of one or more of the figures in this paper are available online at http://ieeexplore.ieee.org.

Digital Object Identifier 10.1109/TIE.2012.2198036

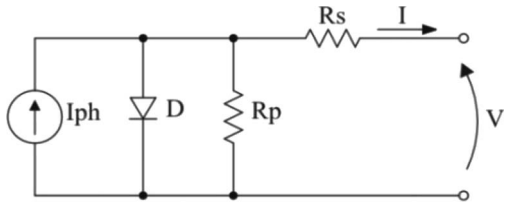

Fig. 2. Equivalent model of the PV panel.

that other papers related to comparisons of MPPT algorithms can be found in the literature [22]–[26]. However, this paper presents additional comparisons about the MPPT algorithms, their flowcharts, more interesting experimental results, and the improved modified MPPT proportional–integral (PI)-based IC and perturb and observe (P&O) methods, which presented outstanding performances because of their inherent adaptative capabilities. Finally, experimental results with typical daily power profile are not found in the literature for so many MPPT methods.

II. PV Panel Modeling

The equivalent circuitry of a PV cell is shown in Fig. 2, in which the simplest model can be represented by a current source in antiparallel with a diode and the nonidealities are represented by the insertion of the resistances Rs (series resistance) and Rp (parallel resistance).

The PV panel simulation model is based on the output current of one PV equivalent model, and its mathematical equation is represented by

$$I = I_{\rm ph} - I_r \cdot \left[e^{q\cdot(V+I\cdot R_s)/\eta\cdot k\cdot T} - 1\right] - \frac{V + I\cdot R_s}{R_p} \qquad (1)$$

where V represents the output PV voltage of one PV panel, $I_{\rm ph}$ is the photocurrent, I_r is the saturation current, q is the electrical charge $(1.6 \times 10^{-19}$ C), η is the p-n junction quality factor, k is the Boltzmann constant $(1.38 \times 10^{-23}$ J/K), and T is the temperature (in kelvins).

Equation (1) can be modified in order to present a null root when current I approaches the real PV current. So, (1) became (2) as a function of its own PV current

$$f(I) = I_{\rm ph} - I - I_r \cdot \left[e^{\frac{q\cdot(V+I\cdot R_s)}{\eta\cdot k\cdot T}} - 1\right] - \frac{V + I\cdot R_s}{R_p}. \qquad (2)$$

Current I, with a null initial value, is utilized in an iterative process that approximates (2) of its root, being obtained by the Newton–Rhapson method (3), which seeks the zero of the differentiable function

$$x_{n+1} = x_n - \frac{f(x_n)}{f'(x_n)}. \qquad (3)$$

Thus, the derivative of (2) is presented in

$$f(I) = -1 - I_r \cdot \left[e^{q\cdot(V+I\cdot R_s)/\eta\cdot k\cdot T}\right] \frac{q\cdot R_s}{\eta\cdot k\cdot T} - \frac{R_s}{R_p}. \qquad (4)$$

With the aforementioned equations, an embedded function to simulate the PV panel in MatLab/Simulink was created.

TABLE I
ELECTRICAL PARAMETERS OF THE PV CELL

Maximum Power	P_{max} = 200Wp
Voltage at MPP	V_{MPP} = 26.3V
Current at MPP	I_{MPP} = 7.61A
Open Circuit Voltage	V_{oc}= 32.9V
Short Circuit Current	I_{sc} = 8.21A
Temperature Coefficient of I_{sc}	$\alpha = 3.18\text{x}10^{-3}$A/°C

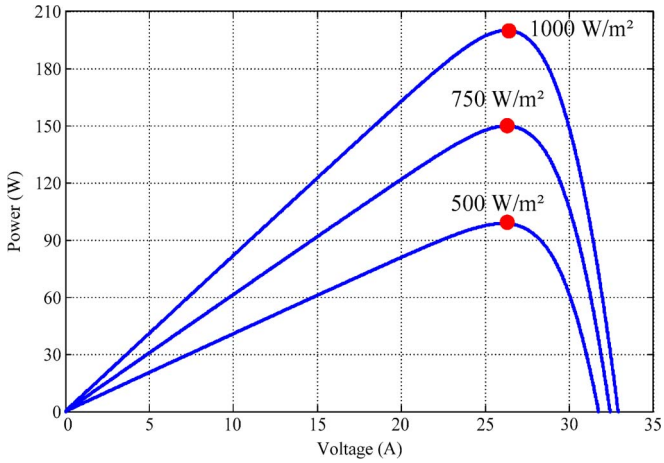

Fig. 3. PV power characteristic for different irradiation levels.

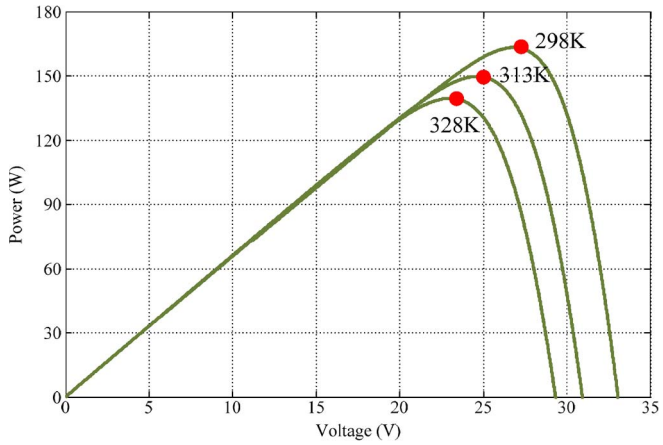

Fig. 4. PV power characteristic for different temperature levels.

The model was used as a voltage source, and the integrator represents the capacitance that stores the injected current from the PV panel. The PV electrical parameters are presented in Table I.

In Figs. 3 and 4, the power characteristics of the analyzed PV cell, considering solar irradiation and temperature changes, are shown. The curves show clearly the nonlinear characteristics, and they are strongly influenced by climate changes.

III. Main MPPT Techniques

A. Fixed Duty Cycle

The fixed duty cycle represents the simplest of the methods, and it does not require any feedback, where the load impedance is adjusted only once for the MPP.

B. CV Method

The constant voltage (CV) method uses empirical results, indicating that the voltage at MPP (V_{MPP}) is around 70%–80% of the PV open-circuit voltage (V_{OC}), for the standard atmospheric condition. Among the points of MPP (varying atmospheric conditions), the voltage at the terminals of the module varies very little even when the intensity of solar radiation changes, but it varies when the temperature changes. So, this method must be used in regions where the temperature varies very little. A positive point is that only the PV voltage is necessary to be measured, and a simple control loop can reach the MPP [4], [5], [21], [22].

C. MPP Locus Characterization

The basic idea of this method is to find a linear relationship between voltage and current at the MPP (MPP locus). This relationship is the tangent line to the MPP locus curve for the PV current in which the minimum irradiation condition satisfies the sensitivity of the method. The equation that guides this method is given by (5). It should be informed that the mathematical derivation is found in [6]. As one can observe, it is hard to obtain all the necessary parameters, and a linear approximation is made offline with the PV panel, translating it as an estimation method. As the MPP locus varies with temperature, the model needs to be updated. This is done by measuring the open-circuit voltage periodically, which means that the interface converter must open the PV circuit, resulting in loss of power in these instants. This MPPT method works better for high solar irradiations [6]

$$T_L = \left(\frac{\eta \cdot V_T}{I_{\mathrm{MPP}}} - N \cdot R_s\right) \cdot I_{\mathrm{MPP}} + \{V_{oc} - \eta[VD_o + V_T]\} \tag{5}$$

where N is the number of cells, I_{MPP} is the current at MPP, V_T is the temperature voltage, and VD_o is the differential voltage [6].

D. P&O and P&O Based on PI

The P&O method operates by periodically incrementing or decrementing the output terminal voltage of the PV cell and comparing the power obtained in the current cycle with the power of the previous one (performs dP/dV). If the voltage varies and the power increases, the control system changes the operating point in that direction; otherwise, it changes the operating point in the opposite direction. Once the direction for the change of voltage is known, the voltage is varied at a constant rate. This rate is a parameter that should be adjusted to allow the balance between faster response and less fluctuation in steady state [5], [7], [18], [21]–[24]. A modified version is obtained when the steps are changed according to the distance of the MPP, resulting in higher efficiency. This is an excellent method to reach the MPP, and it is independent from the PV panel/manufacturer; however, this method may suffer from fast changes in environmental conditions. Interesting P&O algorithm comparisons can be found in [8]. The implementation

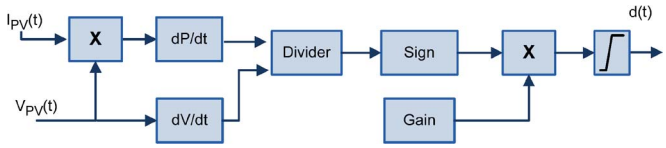

Fig. 5. Implementation of P&O method through MatLab/Simulink.

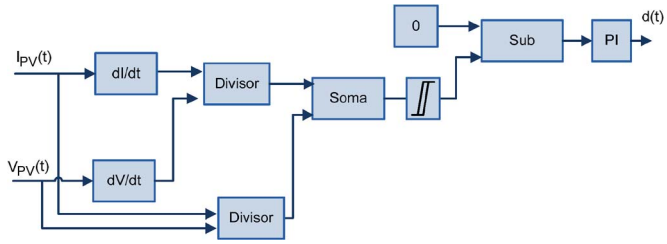

Fig. 6. Implementation of IC method using PI controller.

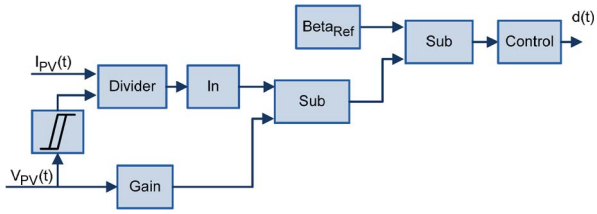

Fig. 7. Implementation of the beta method.

of P&O method using Simulink is shown in Fig. 5, and the following equation represents this method:

$$signal\left(\frac{dP}{dV}\right) \times (-kr) = d \tag{6}$$

where dP/dV represents the derivative of P in relation to V, kr is a constant, and d is the duty cycle.

Improvements can be obtained through a digital controller, transforming the conventional P&O into an adaptive solution once different step sizes according to the distance of the MPP are performed. In steady state, the operation point is not altered unless changes in environmental conditions happen. The key idea is to reduce to zero the dP/dV using a closed-loop control performing the P&O based on PI.

E. IC and IC Based on PI

The IC method is based on the fact that the power slope of the PV is null at MPP ($dP/dV = 0$), positive in the left, and negative in the right, as shown in Fig. 4 [8], [9], [22]–[25]. Thus, due to this condition, the MPP can be found in terms of the increment in the array conductance. Using (7), it is possible to find the IC conditions presented by (8)

$$\frac{dp}{dv} = \frac{d(v \times i)}{dv} = i + v\frac{di}{dv} = 0 \tag{7}$$

$$\frac{\Delta i}{\Delta v} = -\frac{i}{v} \quad \text{(a)}$$

$$\frac{\Delta i}{\Delta v} > \frac{i}{v} \quad \text{(b)}$$

$$\frac{\Delta i}{\Delta v} < \frac{i}{v} \quad \text{(c)} \tag{8}$$

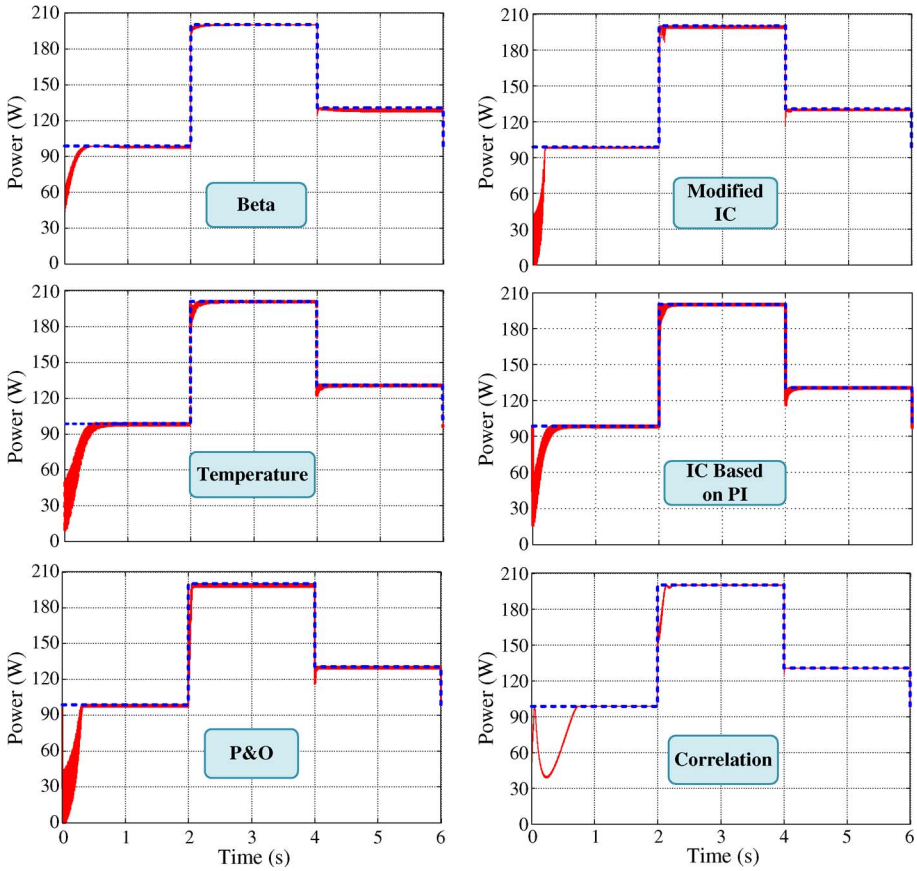

Fig. 8. Power extracted from PV cell with the best MPPT techniques.

where (a) represents the condition at MPP, (b) represents the condition in the left of MPP, and (c) represents the condition in the right of MPP.

In theory, the steady-state oscillations would be eliminated once the derivative of power with respect to voltage is null at MPP. However, a null value of this slope hardly ever occurs due to digital implementation resolution. Strong points are that this method also features a modified version and does not suffer from fast transients in environmental conditions [10], [11]. The IC method needs to monitor both the voltage and current of the PV as P&O method. However, it is not necessary to calculate the PV power. A contribution in the implementation of this method can be done by adding a simple PI controller to improve the IC method, minimizing the error between the actual conductance and the incremental conductance, because the compensator can be adjusted and updated according to the system necessity. Thus, the implementation of IC method by means of a PI controller can be visualized in Fig. 6, using (6) and (7). Moreover, this PI controller can reduce the ripple oscillations in steady state, minimizing the issues involving digital resolution implementation. This method can be seen as an adaptative solution once it presents large step sizes when the PV is far from the MPP; then, the step sizes are reduced according to the distance of MPP, and finally, when the MPP is achieved, the system operation point is not changed, unless the climate conditions are modified. The digital PI can control directly the duty cycle (d) or the converter current (IL). With both constraints, it is possible to find the MPP. Using IL rather than d, it makes the control more attractive once it permits that great changes in environmental conditions can be described as small changes in the converter current; however, if d is the control action, great changes means big changes in the operation point of the converter. Thus, the controller bandwidth must be reduced in the second case.

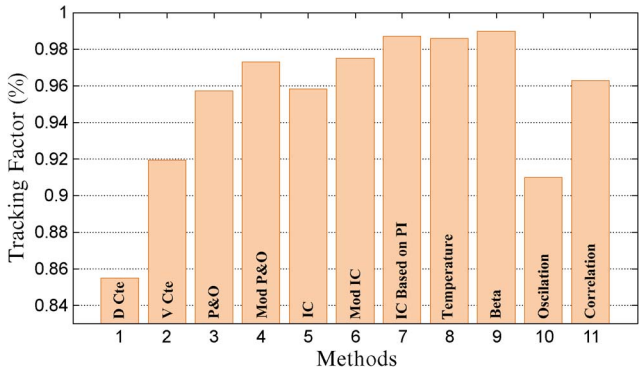

Fig. 9. Percent of energy extracted from the PV panel—TF.

F. Beta Method

The beta method is the approximation of the point of maximum power through the equation of an intermediate variable β, as given in the following [12]:

$$\beta = \ln\left(\frac{I_{\mathrm{PV}}}{V_{\mathrm{PV}}}\right) - c \times V_{\mathrm{PV}} \tag{9}$$

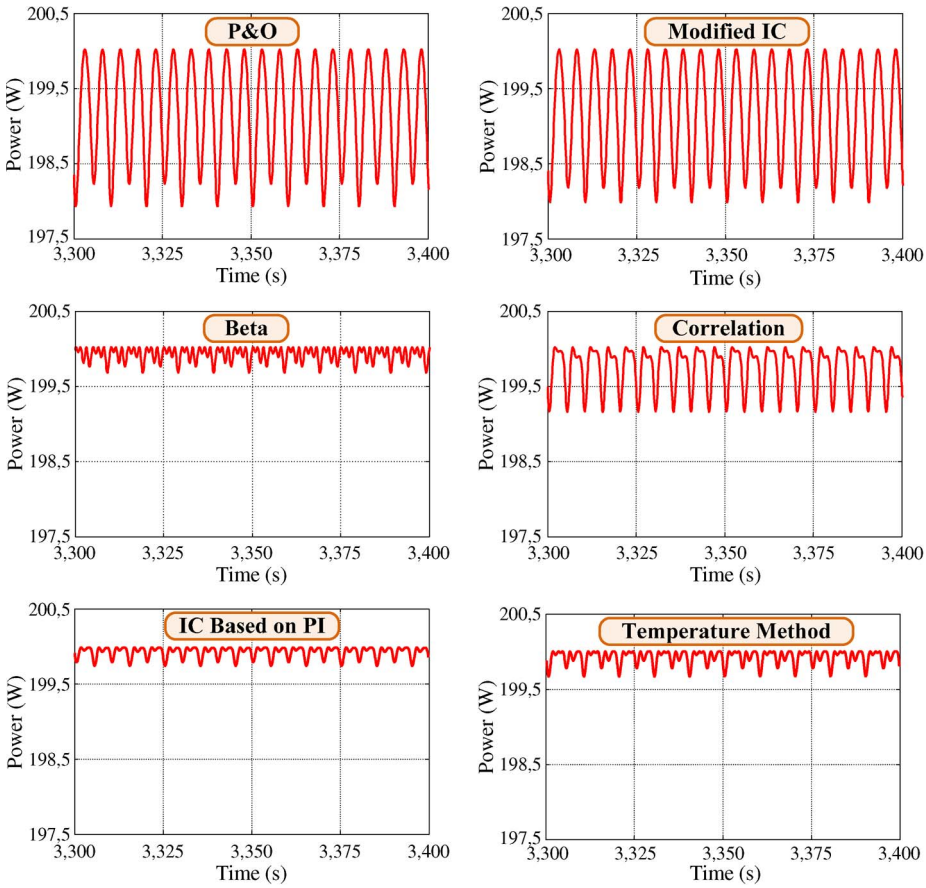

Fig. 10. Power ripple in steady state (approximately 200 Wp).

where $c = (q/(\eta \cdot K_B \cdot T \cdot Ns))$ is a constant that depends on the electron charge (q), the quality factor of the junction panel (η), the Boltzmann constant (K_B), temperature (T), and amount of series PV cells (Ns).

Moreover, as the operating conditions change, the value of β at the optimum point remains almost constant. Thus, β can be continuously calculated using the voltage and current of the panel and inserted on a conventional closed loop with a constant reference [12]. However, for optimal performance, it is mandatory to know the PV electrical parameters, which can reduce the attractiveness of this method. The implementation of this method is shown in Fig. 7.

G. System Oscillation and Ripple Correlation

The system oscillation method is based on the principle of maximum power transfer, and it uses the oscillations to determine the optimum point of operation. At the MPP, the ratio of the amplitude of the oscillation to the average voltage is constant. This method needs only to sense PV voltage, and it can be easily implemented with only analogical circuitries [13], [14]. Its implementation is basically characterized by the usage of filters. For implementing system oscillation, the double grid frequency (in the case of grid-tied converters) or the additional low-frequency ripple can be used. However, switching frequencies must be filtered before being acquired in order to avoid wrong switching states and an increase of electromagnetic interference issues, and because of that, implementation of this method in the converter switching frequency is not a common option. Ripple correlation is also based on the principles of maximum power transfer, and it uses the oscillations in power through all pass filters to obtain the optimal point. In other words, the high-frequency ripples in power and voltage are captured using high-frequency filters, which are used to compute dP/dV. Then, the sign of this derivative is used in a signal function to indicate the right region of operation, and an integrator also ensures the MPP. Additionally, this method presents very fast dynamics converging asymptotically to the MPP, and it is also possible to achieve convergent speeds at a rate similar to the switching converter frequency; however, it is limited by the converter controller gain [15], [16].

H. Temperature Method

Another very good option is to use a temperature method where the shortcomings of variations in temperature, which strictly changes the MPP, can be avoided. For this purpose, a low-cost temperature sensor is adopted and modifies the MPP algorithm function, maintaining the right track of MPP. However, temperature sensing in practical implementations can be a problematic issue due to irregular distribution of PV array temperature, which can be avoided in small PV converters. Moreover, the sensor may be poorly calibrated or not correctly attached, providing wrong measurements of PV temperature.

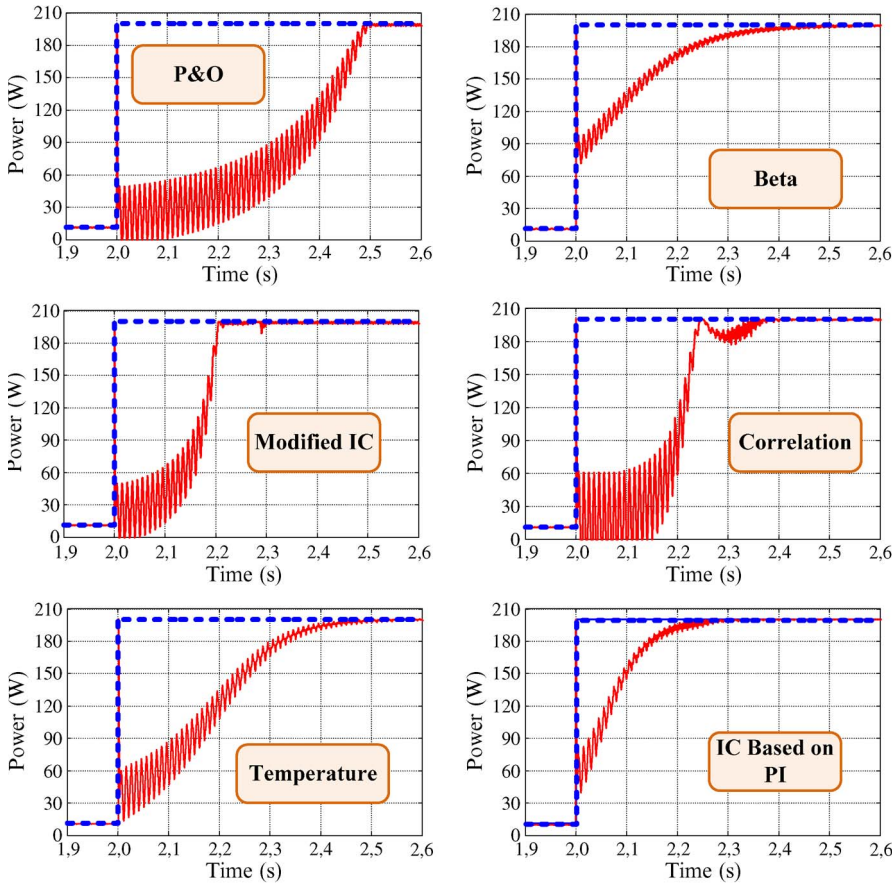

Fig. 11. MPPT dynamic behavior (10–200-W step change).

This method is similar to the Vcte method, and because of that, it is simple for implementation [17], [19]–[21]. The equation that guides the temperature method is presented in

$$V_{\mathrm{MPP}}(t) = V_{\mathrm{MPP}}(T_{\mathrm{ref}}) + T_{\mathrm{Kvoc}}(T - T_{\mathrm{ref}}) \qquad (10)$$

where V_{MPP} is the MPP voltage, T is the panel temperature surface, T_{Kvoc} is the temperature coefficient of V_{MPP}, and T_{ref} is the standard test conditions temperature.

IV. Simulation Results

The average model of the boost dc–dc converter was used to simulate the load variation controlled via MatLab/Simulink and was added a fluctuation (low-frequency ripple) in the average model to permit system oscillation MPPT tests. All tests were performed considering the same temperature and irradiation steps. All algorithms were tuned for its best efficiency, i.e., step sizes (or gains) were increased until reaching this condition; surpassing it, TF is reduced. Fig. 8 shows the responses of some best MPPT algorithms evaluated, where the maximum power is highlighted in blue and the graph in red is the PV power extracted. The simulation setup includes a boost inductor of 2.5 mH, an output capacitor of 36 μF, and a load of 50 Ω. Table I summarizes the PV characteristics.

Aiming to compare and adjust appropriately each algorithm according to the application, it becomes necessary to provide performance measures that can be used as comparison criteria.

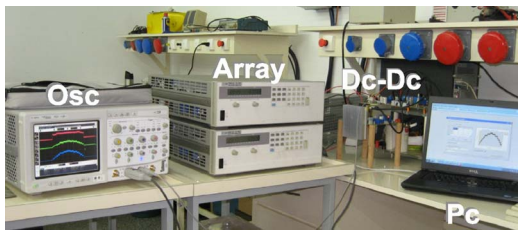

Fig. 12. Experimental arrangement—laboratory setup.

Beyond the typical measures of dynamic responses, there are also additional metrics that are used in these cases. Because the transmitted energy is essential for the use of PV cell as an energy source, a very important measure is the TF, which is the percentage of available energy that was converted. The ripple voltage in steady state is also of vital importance, as there is a limit of ripple so that the panel will remain effective at the MPP. For the MPPT algorithm to reach 98% of the power extracted, the ripple voltage at MPP should not exceed 8.5% [27].

Other factors such as ease of implementation, number of sensors, and cost are also desirable. The TF is shown in Fig. 9, and according to it, the P&O modified and IC modified, IC based on PI, ripple correlation, temperature, and beta methods stand out, and the beta and IC based on PI methods can extract the greatest amount of energy from the PV, being on the order of 98.5% and 98.3%, respectively.

Ripple comparisons in steady state of the power extracted are shown in Fig. 10, where beta, IC based on PI, and temperature

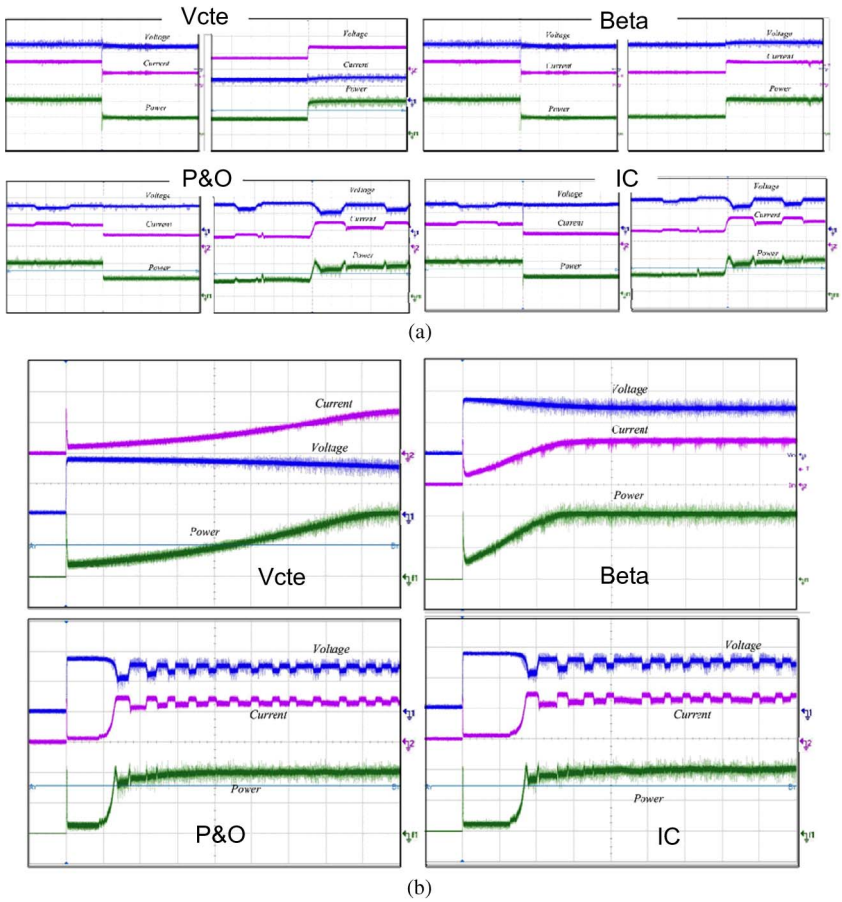

Fig. 13. Dynamic behavior of MPPT methods. (a) Steps (200–100 W) and (100–200 W). (b) Initialization (0–200 W). Scales: Voltage (20 V/div), current (5 A/div), power (100 W/div), and time [(a) 20 and (b) 200 ms/div].

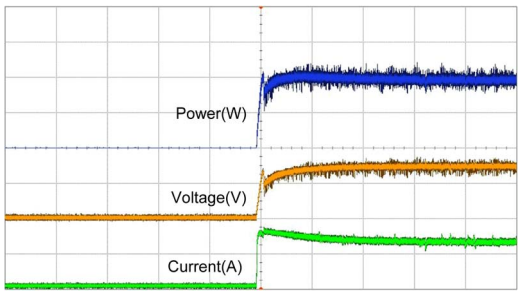

Fig. 14. Initialization of ripple correlation method. Scales: Power (100 W/div), voltage (20 V/div), current (5 A/div), and time (20 ms/div).

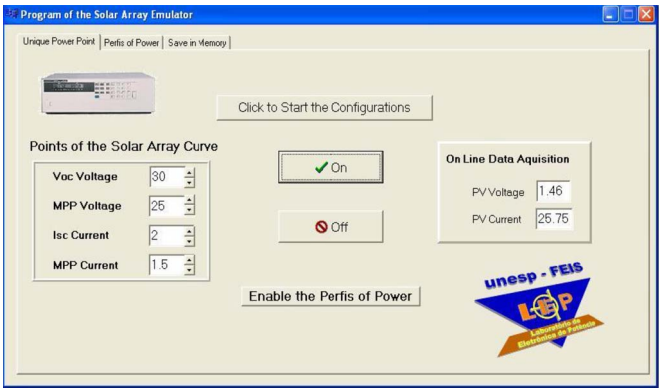

Fig. 15. User-friendly graphical interface—unique operation point.

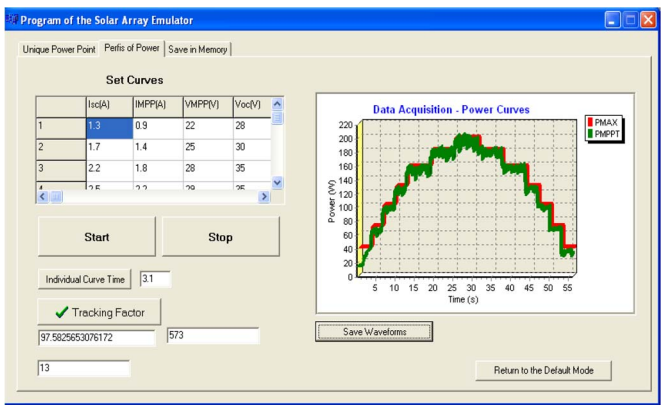

Fig. 16. User-friendly graphical interface—power profile.

methods stand out for having the slightest ripple in steady state. The MPPT methods should also be compared with respect to their dynamic response, i.e., how they behave when the power panel is minimal and quickly changed to the nominal condition. Just to test, the resulting degree of power varies instantaneously from 10 to 200 W, and it can be evaluated using Fig. 11. According to these results, the IC based on PI, ripple correlation, and modified IC methods stand out, and it is the modified IC method which presents less time to reach the steady state. This occurred once the modified IC could be tuned to present the biggest step size when the PV was far from the

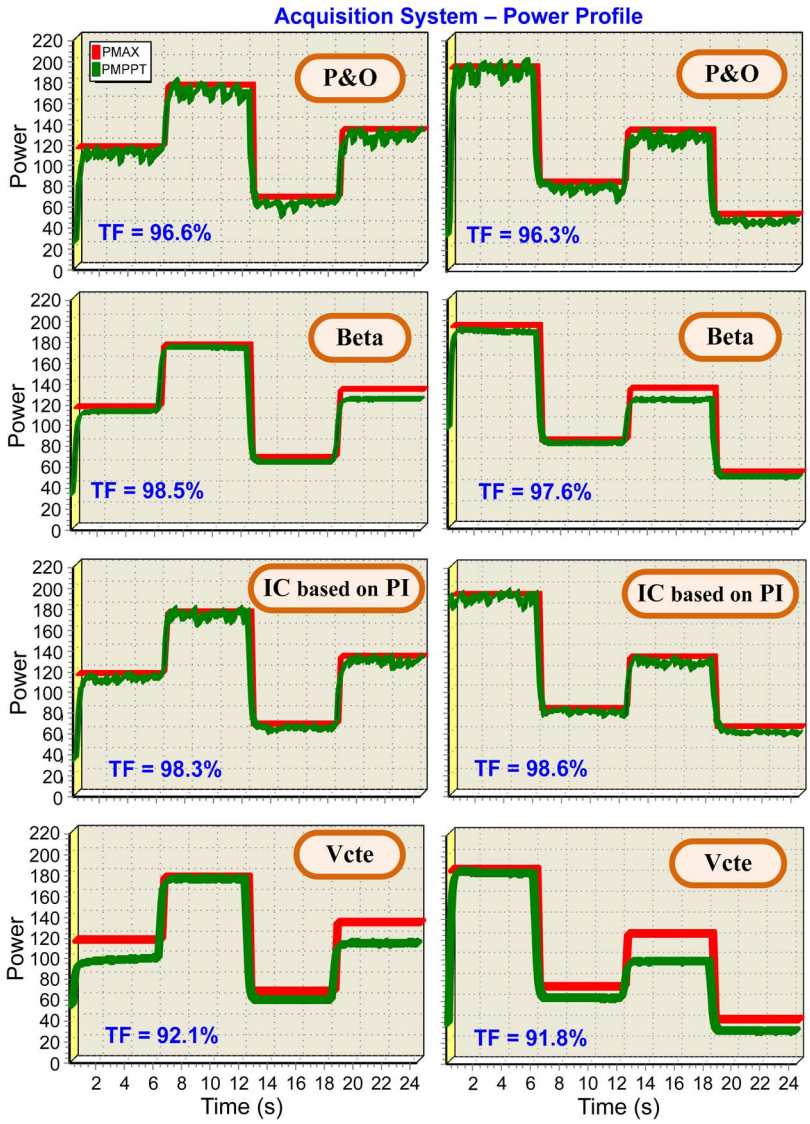

Fig. 17. Experimental power extracted for the MPPT methods.

MPP. Just to highlight, the IC and P&O methods had the same indices of quality, since they are based on the same principle of searching for MPPT, which is dP/dV null at MPP [28].

V. Experimental Results

The implemented prototype and the experimental arrangement are shown in Fig. 12, being composed by oscilloscope, solar array emulators, converter, and personal computer.

The algorithms were digitally implemented in the dSPACE ACE1104 platform, which emulates a DSP TMS320F240 core, and the main results are presented in this section. The irradiation and temperature steps are configurable using the Agilent E4350B PV emulator. The boost dc–dc converter operates with a switching frequency of 50 kHz while the control system presents a sampling rate of 10 kHz.

It is possible to verify the beta method, CV, P&O, and IC dynamic responses in Fig. 13. According to the dynamic responses, the evaluated methods presented very good performances. All of them changed the PV output power in less than 20 ms when submitted to a power change (100–200 W and vice versa). Only the CV method presented a poor initialization time, spending 1.6 s to reach the MPP from the OFF state. The beta method presented a good initialization time, which is approximately 500 ms. Experimentally, the initialization of P&O and IC methods stands out, but the on-time perturbations represent loss of power in steady state.

Among the evaluated MPPT algorithms, ripple correlation presented the best initialization time, i.e., time on the order of 50 ms to reach the maximum power from zero state. This dynamic behavior can be easily verified in Fig. 14. This method was tuned to allow its best performance, and it stands out because it can present a dynamic performance close to the switching converter frequency, but being limited by the converter controllers' gain.

In order to facilitate the experimental evaluations and compute the TF, an acquisition management system was implemented using C++ Builder. The PC user-friendly graphical interface can be visualized in Figs. 15 and 16. Using this system was possible to remotely program the array emulator with a set

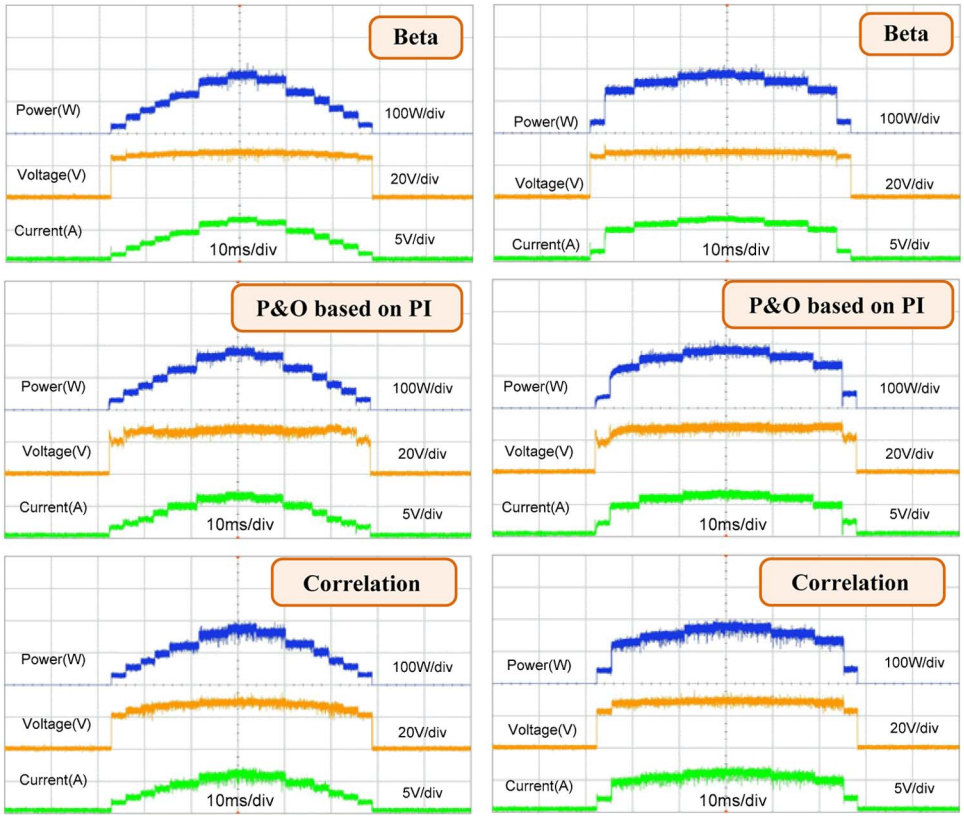

Fig. 18. Similar daily insulation and temperature power profiles—oscilloscope acquisition. Right waveforms suppose sun tracker use.

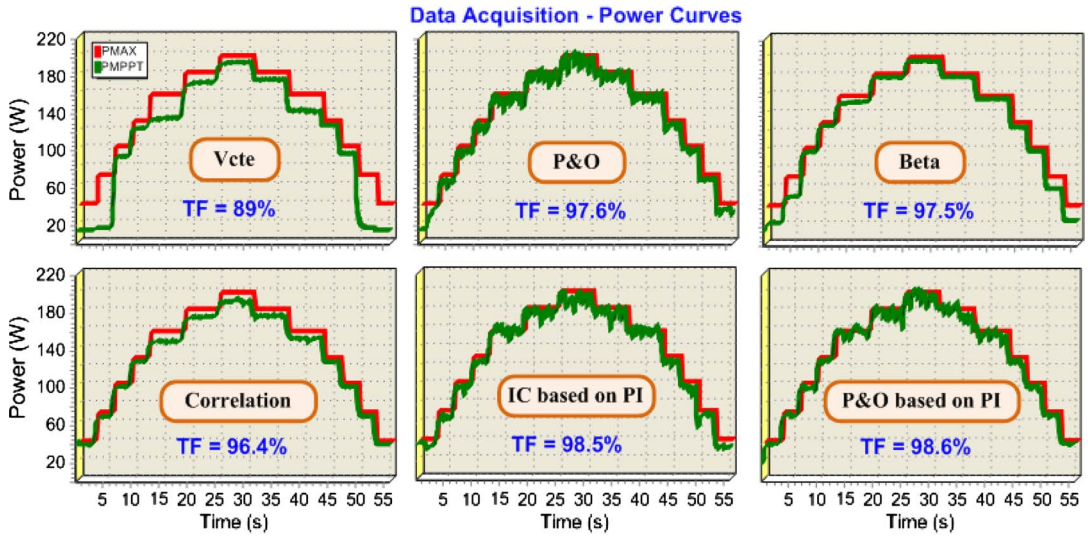

Fig. 19. Similar daily insulation and temperature profiles—computed TF.

of irradiation and temperature curves forming power profiles. The communication was made via General Purpose Interface Bus-Universal Serial Bus to exchange data from computer and array emulator. The evaluation of extracted power can be observed in Fig. 17, where P_{MAX} represents the maximum available power and P_{MPPT} represents the energy converted. Similar profiles of a typical daily insulation were applied, as shown in Figs. 18 and 19, and a good response to these profiles represent a greater gain in relation to the study of the ability of energy extraction in the face of real conditions. It was supposed to simulate the daily characteristics, i.e., the power profile not the total time, from 6 A.M. to 6 P.M. Finally, Table II summarizes the major characteristics of the analyzed MPPT algorithms. During the experimental evaluations, the P&O algorithm was also implemented using a digital PI controller, performing the adaptative P&O based on PI method. Similar to the adaptative IC, this P&O implementation presented more interesting results regarding the higher TF and reduced oscillations in steady state. Thus, this MPPT algorithm was also submitted to the same daily power profile, and the results can be seen in Figs. 18 and 19. The higher TF can be understood once the digital controller performs bigger step sizes when

TABLE II
MAJOR CHARACTERISTICS OF MPPT ALGORITHMS

Method	Dependency of PV Array	Tracking Factor (TF)	Implementation	Accurate	Sensors
Dcte	No	Poor	Very Simple	No	-
Vcte	Yes	Reasonable	Simple	No	V
P&O	No	Good	Simple	Yes	V,I
IC	No	Good	Medium	Yes	V,I
Modified P&O	No	Very Good	Complex	Yes	V,I
P&O based on PI	No	Excellent	Medium	Yes	V,I
Modified IC	No	Very Good	Complex	Yes	V,I
IC based on PI	No	Excellent	Medium	Yes	V,I
Beta	Yes	Excellent	Medium	Yes	V,I
System Oscillation	Yes	Reasonable	Simple	No	V
Ripple Correlation	No	Good	Complex	Yes	V,I
Temperature	Yes	Very Good	Simple	Yes	V, Temperature

PV is far from the MPP, and when it is achieved, the steps are reduced, minimizing the losses of power in steady state.

VI. SYSTEMS UNDER PARTIAL SHADING

Most of the aforementioned MPPT methods presented very good indices of quality in all studied aspects, being extremely useful in the field of photovoltaics cells. Their performances are guaranteed for the use with microinverters (single PV cell) or with midinverters with few series connections of PV modules (close and with the same sun inclination) in places where the environmental conditions are uniform most of the time; that happens in tropical places, as an example. Nevertheless, it is not a rule for all regions and for series–parallel connections of several PV modules. So, these algorithms must be updated to track the global MPPT instead of the local MPPT, in the case of shading phenomena [29]–[32]. It can be done by adding a first stage before applying the appropriate algorithm. From the employed ideas, the step-by-step scan of PV curve is a good choice and dependent upon the step sizes but independent of the PV array. The PV voltage is varied, for example, from the open-circuit voltage until a percentage of its voltage, and the voltage at the global MPP is saved in a memory. After finding this point, the MPPT algorithm is performed to constantly track the MPP. In order to reduce the quantity of steps to find the true MPP, a current-controlled converter is used to increment the PV power [29], or the local maxima are found before; then, right and left steps are applied constantly to find the global point [31]. This global MPPT search must be performed constantly in order not to lose the global MPP. Time intervals of 10–15 min are used to perform this search. The TF reduction is insignificant in comparison to the amount of energy that can be harvested [29].

VII. CONCLUSION

Currently, the usage of energy from PV panels is a reality, and its intensive use will become extremely important in finding solutions to energy and environmental problems very soon. In this context, the used MPPT techniques are the most important to extract the maximum power available in PV. Among the methods evaluated, the beta method was presented as a good solution regarding high-quality TF, reduced and smaller ripple voltage in steady state, good transient performance, and medium complexity of implementation; however, it is dependent on the PV characteristics. It is noted that the modified IC, modified P&O, IC based on PI, and P&O based on PI methods also deserve mention as alternatives for outstanding performance, which are independent from the type/manufacturer of the PV panel, with the IC based on PI and P&O based on PI methods having the best TFs even in the face of more realistic daily power profiles and also presenting very good transient performance. However, it is not easy to perform division functions, and in this case, the digital implementation is desirable.

The idea of implementing the MPPT algorithms through digital controllers can be applied to all methods if it were possible to minimize error functions.

It is interesting to point out that the differences in performances among the best analyzed MPPTs are very slight, and these algorithms must be evaluated according to each situation. Nevertheless, this paper contributes as a good guide for choosing which algorithm should be implemented. Finally, it should be pointed out that, in the case of cost reduction, it is interesting to take in mind the temperature method. In the case of intensive shading, the aforementioned algorithms are interesting choices for the second stage of the MPP track.

REFERENCES

[1] C. Wolfsegger and J. Stierstorfer, *Solar Generation IV: Solar Electricity for Over One Billion People and Two Million Jobs by 2020*. Amsterdam, The Netherlands: Greenpeace, 2007, EPIA.
[2] European Renewable Energy Council, EREC-2005. [Online]. Available: http://www.erec.org/renewable-energy/photovoltaics.html
[3] J.-M. Kwon, K.-H. Nam, and B.-H. Kwon, "Photovoltaic power conditioning system with line connection," *IEEE Trans. Ind. Electron.*, vol. 53, no. 5, pp. 1048–1054, Jun. 2006.
[4] A. Pandey, N. Dasgupta, and A. K. Mukerjee, "A simple single-sensor MPPT solution," *IEEE Trans. Power Electron.*, vol. 22, no. 6, pp. 698–700, Mar. 2007.

[5] W. Li, Y. Zheng, W. Li, Y. Zhao, and X. He, "A smart and simple PV charger for portable applications," in *Proc. APEC*, 2010, vol. 25, pp. 2080–2084.
[6] V. V. R. Scarpa, S. Buzo, and G. Spiazzi, "Low complexity MPPT technique exploiting the effect of the PV Module MPP Locus characterization," *IEEE Trans. Ind. Electron.*, vol. 56, no. 5, pp. 1531–1538, May 2009.
[7] W. L. Yu, T.-P. Lee, G.-H. Wu, Q. S. Chen, H.-J. Chiu, Y.-K. Lo, and F. Shih, "A DSP-based single-stage maximum power point tracking PV inverter," in *Proc. APEC*, 2010, vol. 25, pp. 948–952.
[8] A. K. Abdelsalam, A. M. Massoud, S. Ahmed, and P. N. Enjeti, "High-performance adaptive perturb and observe MPPT technique for photovoltaic-based microgrids," *IEEE Trans. Power Electron.*, vol. 26, no. 4, pp. 1010–1021, Apr. 2011.
[9] G. C. Hsieh, H.-L. Chen, Y. Chen, C.-M. Tsai, and S.-S. Shyu, "Variable frequency controlled incremental conductance derived MPPT photovoltaic stand-along DC bus system," in *Proc. APEC*, 2008, vol. 23, pp. 1849–1854.
[10] R. A. Mastromauro, M. Liserre, T. Kerekes, and A. Dell'aquila, "A single-phase voltage-controlled grid-connected photovoltaic system with power quality conditioner functionality," *IEEE Trans. Ind. Electron.*, vol. 56, no. 11, pp. 4436–4444, Nov. 2009.
[11] F. Liu, S. Duan, F. Liu, B. Liu, and Y. Kang, "A variable step size INC MPPT method for PV systems," *IEEE Trans. Ind. Electron.*, vol. 55, no. 7, pp. 2622–2628, Jul. 2008.
[12] S. Jain and V. Agarwal, "A new algorithm for rapid tracking of approximate maximum power point in photovoltaic systems," *IEEE Power Electron. Lett.*, vol. 2, no. 1, pp. 16–19, Mar. 2004.
[13] B. M. T. Ho, H. S. H. Chung, and W. L. Lo, "Use of system oscillation to locate the MPP of PV panels," *IEEE Power Electron. Lett.*, vol. 2, no. 1, pp. 1–5, Mar. 2004.
[14] B. M. Ho and H. S. Chung, "An integrated inverter with maximum power tracking for grid-connected PV systems," *IEEE Trans. Power Electron.*, vol. 20, no. 4, pp. 953–962, Jul. 2005.
[15] D. Casadei, G. Grandi, and C. Rossi, "Single-phase single-stage photovoltaic generation system based on a ripple correlation control maximum power point tracking," *IEEE Trans. Energy Convers.*, vol. 21, no. 2, pp. 562–568, Jun. 2006.
[16] T. Esram, J. W. Kimball, P. T. Krein, P. L. Chapman, and P. Midya, "Dynamic maximum power point tracking of photovoltaic arrays using ripple correlation control," *IEEE Trans. Power Electron.*, vol. 21, no. 5, pp. 1282–1291, Sep. 2006.
[17] M. Park and I. A. Yu, "Study on the optimal voltage for MPPT obtained by surface temperature of solar cell," in *Proc. IECON*, 2004, vol. 30, pp. 2040–2045.
[18] N. Femia, G. Petrone, G. Spagnuolo, and M. Vitelli, "Optimization of perturb and observe maximum power point tracking method," *IEEE Trans. Power Electron.*, vol. 20, no. 4, pp. 963–973, Jul. 2005.
[19] N. Mutoh, T. Matuo, K. Okata, and M. Sakai, "Prediction-data-based maximum-power-point-tracking method for photovoltaic power generation systems," in *Proc. IEEE PESC*, 2002, vol. 33, pp. 1489–1894.
[20] R. F. Coelho, F. M. Concer, and D. C. Martins, "A MPPT approach based on temperature measurements applied in PV systems," in *Proc. IEEE ICSET*, 2010, pp. 1–6.
[21] G. J. Yu, Y. S. Jung, I. Choi, and J. H. Song, "A novel two-mode MPPT control algorithm based on comparative study of existing algorithms," in *Proc. PVSC*, 2002, vol. 29, pp. 1531–1534.
[22] R. Faranda, S. Leva, and V. Maugeri, "MPPT techniques for PV systems: Energetic and cost comparison," in *Proc. PESGM*, 2008, vol. 9, pp. 1–6.
[23] M. C. Cavalcanti, K. C. Oliveira, G. M. S. Azevedo, and F. A. S. Neves, "Comparative study of maximum power point tracking techniques for photovoltaic systems," *Eletrôn. Potência*, vol. 12, pp. 163–171, 2007.
[24] T. Esram and P. L. Chapman, "Comparison of photovoltaic array maximum power point tracking techniques," *IEEE Trans. Energy Convers.*, vol. 22, no. 2, pp. 439–449, Jun. 2007.
[25] M. A. G. Brito, L. G. Junior, L. P. Sampaio, and C. A. Canesin, "Evaluation of MPPT techniques for photovoltaic applications," in *Proc. ISIE*, 2011, vol. 20, pp. 1039–1044.
[26] M. Berrera, A. Dolara, R. Faranda, and S. Leva, "Experimental test of seven widely-adopted MPPT algorithms," in *Proc. IEEE Bucharest PowerTech Conf.*, 2009, vol. 8, pp. 1–8.
[27] S. B. Kjaer, J. K. Pedersen, and F. Blaabjerg, "A review of single-phase grid-connected inverters for photovoltaic modules," *IEEE Trans. Ind. Appl.*, vol. 41, no. 5, pp. 1292–1306, Sep./Oct. 2005.
[28] M. Liserre, T. Sauter, and Y. J. Hung, "Future energy systems—Integrating renewable energy sources into the smart power grid through industrial electronics," *IEEE Trans. Ind. Electron.*, vol. 4, no. 1, pp. 18–37, Mar. 2010.
[29] E. Koutroulis and F. Blaabjerg, "A new technique for tracking the global maximum power point of PV arrays operating under partial-shading conditions," *IEEE J. Photovoltaics*, vol. 2, no. 2, pp. 184–190, Apr. 2012.
[30] C. S. Chin, P. Neelakantan, H. P. Yoong, and K. T. K. Teo, "Maximum power point tracking for PV array under partially shaded conditions," in *Proc. CICSyn*, 2011, vol. 30, pp. 72–77.
[31] S. Kazmi, H. Goto, O. Ichinokura, and H. Guo, "An improved and very efficient MPPT controller for PV systems subjected to rapidly varying atmospheric conditions and partial shading," in *Proc. AUPEC*, 2009, pp. 1–6.
[32] R. Alonso, P. Ibanez, V. Martinez, E. Romen, and A. Sanz, "An innovative perturb, observe and check algorithm for partially shaded PV systems," in *Proc. 13th EPE*, 2009, pp. 1–8.

Moacyr Aureliano Gomes de Brito was born in Andradina, Brazil, in 1982. He received the B.S. and M.Sc. degrees in electrical engineering from the Faculdade de Engenharia de Ilha Solteira, São Paulo State University (UNESP), Ilha Solteira, Brazil, in 2005 and 2008, respectively, where he is currently working toward the Ph.D. degree in the Power Electronics Laboratory, working on inverters for stand-alone and grid-connected applications.

His interests include ballasts for fluorescent lamps, dimming control, digital control, dc-to-dc converters, switching-mode power supplies, power-factor-correction techniques, DSPs and field-programmable gate arrays, and stand-alone and grid-connected inverters for photovoltaic applications.

Luigi Galotto, Jr. was born in São Paulo, Brazil, on February 12, 1981. He received the B.S. degree in electrical engineering and the M.S. degree in artificial intelligence applications, with a study on sensor fault-tolerant operation in drive systems from the Federal University of Mato Grosso do Sul (UFMS), Campo Grande, Brazil, in 2003 and 2006, respectively. He received the Ph.D. degree in power electronics at São Paulo State University (UNESP), Ilha Solteira, Brazil, in 2012.

He is also a Researcher at an acknowledged laboratory at UFMS, developing projects in spectrum analyzers, power converters, condition monitoring software, and control systems.

Leonardo Poltronieri Sampaio was born in São José do Rio Preto, Brazil, in 1983. He received the B.Sc. and M.Sc. degrees in electrical engineering from São Paulo State University (UNESP), Ilha Solteira, Brazil, in 2008 and 2010, respectively, where he is currently working toward the Ph.D. degree in electrical engineering.

Since 2000, he has been working on computer programming and Linux operational systems, and he is a member of the Power Electronics Laboratory (LEP), São Paulo State University. His interests include computer programming, education in power electronics, e-learning, education tools, dc–dc converters, inverters, renewable and alternative energy sources, photovoltaic systems, and power electronic converters.

Guilherme de Azevedo e Melo received the B.S., M.S., and Ph.D. degrees in electrical engineering from the Faculdade de Engenharia de Ilha Solteira (FEIS), São Paulo State University (UNESP) Ilha Solteira, Brazil, in 2001, 2006, and 2010, respectively.

Since 2010, he has been a Collaborator Professor with FEIS, UNESP, where he is currently a Member of the Power Electronics Laboratory (LEP).

Dr. Melo's principal interest areas are power electronics, electrical power quality, renewable energy, and control systems.

Carlos Alberto Canesin (S'87–M'97–SM'08) received the B.Sc. degree in electrical engineering from the Faculdade de Engenharia de Ilha Solteira (FEIS), São Paulo State University (UNESP), Ilha Solteira, Brazil, in 1984 and the M.Sc. and Ph.D. degrees in electrical engineering from the Power Electronics Institute, Federal University of Santa Catarina, Florianópolis, Brazil, in 1990 and 1996, respectively.

He started the Power Electronics Laboratory (LEP), FEIS, UNESP, where he is currently a Full Ph.D. Professor. He was the Editor-in-Chief of the *Brazilian Journal of Power Electronics* (in 2003–2004). His interests include power-quality analysis and techniques, active-power-factor-correction techniques, high-power-factor rectifiers, soft-switching techniques, dc-to-dc converters, dc-to-ac converters, switching-mode power supplies, solar/photovoltaic energy applications, electronic fluorescent ballasts, and educational research in power electronics

Dr. Canesin was the President of the Brazilian Power Electronics Society (in November 2004–October 2006). Since 2003, he has been an Associate Editor of the IEEE TRANSACTIONS ON POWER ELECTRONICS, and since 2010, he has been a member of The State of São Paulo Council for Energy Policy (CEPE).